In situ regeneration of retinal pigment epithelium by gene transfer of *E2F2*: a potential strategy for treatment of macular degenerations

Daniel Kampik[1,3], Mark Basche[1], Ulrich FO Luhmann[1,4], Koji M Nishiguchi[1,5], Jennifer AE Williams[2], John Greenwood[2], Stephen E Moss[2], Hong Han[3], Selina Azam[1], Yanai Duran[1], Scott J Robbie[1], James WB Bainbridge[1,6], D Frank Larkin[6], Alexander J Smith[1], Robin R Ali[1,7]

[1]Department of Genetics and [2]Department of Cell Biology, UCL Institute of Ophthalmology, London, UK, [3]University Hospital of Würzburg, Department of Ophthalmology, Würzburg, Germany, [4]Current address: Roche Pharmaceutical Research and Early Development, Ophthalmology Discovery & Biomarkers, Basel, Switzerland, [5]Current address: Department of Advanced Ophthalmic Medicine, Graduate School of Medicine, Tohoku University, Sendai, Japan, [6]Moorfields Eye Hospital, [7]NIHR Biomedical Research Centre at Moorfields Eye Hospital NHS Foundation Trust and UCL Institute of Ophthalmology, London, UK

Correspondence: Robin R. Ali, Department of Genetics, UCL Institute of Ophthalmology, 11-43 Bath Street, London EC1V 9EL, UK, Tel: +44206076817, r.ali@ucl.ac.uk

Short title: *In situ* RPE regeneration by E2F2

Word count: 2843

This work was supported by the National Institute for Health Research Biomedical Research Centre at Moorfields Eye Hospital and UCL and also by Moorfields Eye Charity.

U.F.O.L is currently an employee of F. Hoffmann-La Roche Ltd. All other authors declare that no competing financial interests exist.

Abstract

The retinal pigment epithelium (RPE) interacts closely with photoreceptors to maintain visual function. In degenerative diseases such as Stargardt disease and age-related macular degeneration, the leading cause of blindness in the developed world, RPE cell loss is followed by photoreceptor cell death. RPE cells can proliferate under certain conditions, suggesting an intrinsic regenerative potential, but so far this has not been utilised therapeutically. Here, we used *E2F2* to induce RPE cell replication and thereby regeneration. In both young and old (2 and 18 month) wildtype mice, subretinal injection of non-integrating lentiviral vector expressing E2F2 resulted in 47% of examined RPE cells becoming BrdU positive. E2F2 induced an increase in RPE cell density of 17% compared with control vector-treated and 14% compared with untreated eyes. We also tested this approach in an inducible transgenic mouse model of RPE loss, generated through activation of diphtheria toxin-A gene. *E2F2* expression resulted in a 10-fold increase in BrdU uptake and a 34% increase in central RPE cell density. Although in mice this localised rescue is insufficiently large to be demonstrable by electroretinography, a measure of massed retinal function, these results provide proof-of-concept for a strategy to induce *in situ* regeneration of RPE for the treatment of RPE degeneration.

Introduction

AMD is the leading cause of blindness in the elderly worldwide, affecting 30–50 million individuals, 14 million of which are blind or severely visually impaired.[1-3] Due to the rapidly aging population, the number of persons suffering from advanced forms of AMD will increase by 50% in 2020.[4] Currently, there is neither a preventive or curative treatment for AMD. For non-neovascular AMD affecting the majority of patients (>92%), no established treatment options exist. For neovascular AMD, the most widely used treatment involves administration of antibodies against vascular endothelial growth factor (VEGF) to prevent the formation of new blood vessels. Underlying all forms of AMD is a dysfunctional retinal pigment epithelium (RPE). RPE function is essential for maintaining photoreceptor health by providing growth factors and cytokines[5], forming the outer blood retina barrier, phagocytosis of photoreceptor outer segments and processing retinoids for phototransduction. The continual phagocytosis of shed photoreceptor discs is associated with a high level of oxidative stress that may lead to loss of RPE.[6] The highest turnover rate of shed photoreceptor discs is in the macula where photoreceptor density is highest.[7] In the adult human eye, the RPE is a non-dividing cell system,[8, 9] and death of RPE cells is not compensated by cellular regeneration.[7, 10] In retinal degenerations, when RPE is lost, surrounding RPE cells enlarge to fill the space.[11] This increases metabolic load on individual RPE cells resulting in further damage and loss. Replacing RPE cells by transplantation or inducing controlled proliferation of RPE cells may prevent disease progression.

Various attempts have been made to replace diseased RPE in the central retina, but none so far has proved efficient and safe enough for standard treatment. Macular translocation surgery aims to relocate the central retina to an area of healthy RPE.[12] Despite a high complication rate,[13] gain of visual function in some patients provides a proof-of-concept that RPE re-population under the macula restores vision.[14-17] RPE transplantation, using autologous RPE

sources such as iris pigment epithelium[18] or RPE from the periphery[19-21], has been investigated for over three decades.[22] Recently there have been several clinical trials involving RPE derived from human embryonic stem cells[23] or human induced pluripotent stem cells.[24, 25] Despite promising results, to date there is no consensus over the best method to treat RPE defects and it remains uncertain how effective this approach might be.

Here we propose a new strategy to regenerate RPE *in situ* by making use of its natural proliferative potential. We sought to overcome the intrinsic barriers to RPE proliferation and induce regeneration by mitosis *in vivo* using lentiviral vector-mediated transfer of the gene encoding the transcription factor E2F2, which can induce cells to bypass G1 arrest.[25-27] The E2F transcription factor family and the product of the retinoblastoma tumour suppressor gene (Rb) can be described as opposing molecules that control the G1 to S phase transition,[26] whereby Rb is recognized as a tumour suppressor and key inhibitor of E2F, a central transcriptional activator.[27] The E2F transcription factor family control a variety of genes involved in DNA replication such as thymidine kinase, thymidylate synthase, dihydrofolate reductase – virtually the entire apparatus of initiation factors that assemble a pre-replication complex at the transition from G1 to S phase.[28] While E2F-1 to -4 all induce S phase progression with decreasing efficacy, E2F1 uniquely also induces apoptosis.[29] In this study, we therefore selected E2F2 for overexpression to overcome cell cycle arrest in RPE cells. We test this concept *in vitro*, in wildtype mice and in an inducible RPE-deficient mouse model (RPE^{CreER}/DTA)[11] and provide evidence for *in situ* RPE cell proliferation.

Results and Discussion

The effect of *E2F2* overexpression was assessed *in vitro* on ARPE19 cells. Growth arrested ARPE19 cells, as shown by an absence of nuclear Ki67 **(Fig. S1)**, were transfected with pCMV-E2F2. *E2F2* mRNA persisted at a >1000-fold increase 21 days post transfection **(Fig. 1a)**, inducing E2F2 protein overproduction by 9-fold after 2 days, and 3-fold after 7 days compared with control plasmid **(Fig. 1b,c)**. *E2F2* overexpression coincided with increased protein levels of proliferation marker Cyclin D1 (**Fig. 1b,d)**. Two days after transfection of growth-arrested monolayers with pCMV-E2F2, or control plasmid pcDNA3-EGFP, over 86% of cells were Ki67-positive in both groups. However, on day 7 and 14 post transfection, *E2F2* overexpression resulted in a 2.3-fold and 1.7-fold increase respectively in Ki67-positive nuclei compared with pCDNA3-EGFP controls ($P<0.05$, *t*-test; **Fig. 1e)** suggesting that E2F2 stimulates an increase in proliferation *in vitro*. Similarly, after an initial increase in uptake of bromodeoxyuridine (BrdU), a synthetic thymidine analogue incorporated into newly synthesized DNA, in both control and *E2F2*-transfected cells, BrdU uptake in E2F2-treated cells increased by 3.5- and 5.4-fold, at 1 and 2 weeks respectively, **(Fig. 1f)**. Together these results suggest that *E2F2* overexpression can lead to specific induction of cell proliferation in contact-inhibited ARPE19 cells.

To test whether the same approach might be effective *in vivo*, the *E2F2* construct was packaged into a non-integrating lentiviral vector, LNT-E2F2, and administered subretinally, causing E2F2 overproduction and nuclear localization in the RPE **(Fig. 2a)**. To assess RPE proliferation, 9-week-old wildtype mice received subretinal injections of LNT-E2F2 (2×10^5 infectious particles per eye). Titre matched LNT-hrGFP and medium injected eyes served as controls (n=4). All mice received daily intraperitoneal BrdU injections between day 4-10. On day 10, RPE flatmounts showed co-localized E2F2 and BrdU staining with minimal staining in controls **(Fig. 2b)**. This experiment was repeated twice with different batches of vector and each showed similar results (total n=20, **Fig. S2a)**. In the LNT-E2F2 group **(Fig. 2c)**, a significant linear E2F2/BrdU correlation was observed (Pearson correlation coefficient 0.9170, $P<0.0001$), while no

correlation was observed for the medium-injected control group **(Fig. 2d)**, indicating that uptake of the cell proliferation marker is the effect of *E2F2* overexpression. Compared with the control group, there was a 50-fold increase of E2F2-positive cells in the LNT-E2F2 group, and a 10-fold increase in BrdU-positive cells **(Fig. 2e)**. This experiment was repeated twice with different batches of vector yielding comparable results (total n=20 eyes, **Fig. S2b**). In 18-month-old mice (n=3 mice for pairwise left-right comparison against LNT-hrGFP), we tested whether age of the animal may affect the proliferative effect of *E2F2* overexpression *in vivo*. The similar increase in BrdU uptake upon *E2F2* overexpression in young and 18-month-old mice suggests this approach was not restricted by the age of the recipient **(Fig. 2f)**.

To assess whether the increase in cell proliferation markers resulted in increased RPE cell density, 8-week-old adult mice received subretinal injections of LNT-E2F2, LNT-GFP or medium. Fifty-three phalloidin-stained RPE flatmounts of 30 mice were imaged 10 days after treatment **(Fig. 3a)**. Only transduced areas around the injection site were evaluated; areas directly adjacent to the injection site that were severely dysmorphic were excluded. Compared with controls, LNT-E2F2 treated eyes presented with variable cell size and morphology as would be expected when existing cells divide *in situ* and two new cells take up the available space. It should be noted that the presence of two nuclei constitutes normal morphology for a mouse RPE cell. Cell outlines were partially disrupted and smaller cells gathered in clusters without gaps between cells. No overt pathology of the neuroretina was observed in these eyes. RPE cell density was quantified on masked samples by counting cells outlined by phalloidin staining. Untreated age-matched eyes served as an additional control. One-way ANOVA revealed highly significant differences among groups (P=0.0002, **Fig. 3b**). LNT-E2F2 injected eyes presented an RPE cell density significantly higher that all three control groups (P=0.0011 - 0.0071, Tukey's multiple comparisons test). No significant difference was observed between the control groups (P>0.6). These data reveal that lentiviral-mediated *E2F2* overexpression in the RPE can induce an increase in RPE cell density by about 20% in wildtype RPE.

We next investigated possible effects of LNT-E2F2 injection and the resulting increase in RPE density upon the function of the overlying photoreceptors and gross structure of the neuroretina. As before 8-week-old adult mice received subretinal injections of LNT-E2F2, LNT-GFP or were left uninjected. Retinal function was then assessed by electroretinography (ERG) at 10 and 30 days post injection (DPI) and tissue collected for histological analysis at both timepoints. Analysis of the ERG data revealed no significant differences between the LNT-E2F2 and LNT-eGFP treated groups at either timepoint under both photopic **(Fig. S3a)** and scotopic **(Fig. S3b)** conditions. Additionally, histological assessment of neuroretina revealed no apparent differences in retinal morphology between the injected groups at either timepoint **(Fig. S3c).** In all examined eyes, retinal morphology appeared normal.

To test whether E2F2 overexpression can also increase cell density in diseased RPE, we assessed LNT-E2F2 administration in double-transgenic RPE^{CreER}/DTA mice. These carry a tamoxifen-inducible Cre recombinase driven by the RPE-specific monocarboxylate transporter 3 (*SLC16A8)* promoter, and a diphtheria toxin A chain (DTA) gene rendered transcriptionally silent by a floxed stop sequence. Activation of Cre by tamoxifen injection induces DTA expression, causing partial RPE cell loss. Four double transgenic $RPE^{CreER\ +/-}$/$DTA^{+/-}$ and four wildtype mice received intraperitoneal tamoxifen injections (postnatal days 12–24) to induce RPE ablation in the transgenic mice only. At four months of age, RPE showed polymorphous cells with increased cell size compared to wildtype RPE, but the monolayer remained intact without holes **(Fig. 4a)**. Mean cell density was reduced by 15±5% (P=0.0082, **Fig. 4b)**. Regional analysis revealed that the reduction in cell density in transgenic compared to wildtype mice was most pronounced in the central RPE, where there was a 24±10% decrease (P=0.0231, **Fig. 4c)**, in line with our previous findings.[11]

RPE damage was induced in 4 transgenic mice as described above. At 4 months, treatment vector LNT-E2F2 and control vector LNT-GFP were injected subretinally into right and left eyes,

respectively. Animals received intraperitoneal BrdU injections daily from day 4 to day 10 afterwards. On day 10, RPE-choroid-sclera complexes were immunostained for BrdU and ZO-1 and flatmounted. We analysed both treated and untreated areas, i.e. areas outside the injection bleb, of the flatmounts throughout all eyes of both groups, as shown schematically in **Fig. 5a** (injection sites were excluded). In RPE^{CreER}/DTA transgenic LNT-E2F2 treated eyes, we observed BrdU uptake comparable with wildtype C57BL6/J mice after LNT-E2F2 treatment, while LNT-GFP injected control eyes showed almost no BrdU uptake **(Fig. 5b,c)**. LNT-E2F2 treatment of RPE^{CreER}/DTA mice increased BrdU uptake by 9-fold±3.4 (mean ±SD, P=0.0173, paired t-test, n=4 eyes). Following LNT-E2F2 treatment, overall cell density was increased 20±11% (mean ±SEM) compared with control vector. However, this did not reach statistical significance (P=0.2043, unpaired t-test). Regional analysis revealed that the largest increase in cell density was in the centre in RPE ablated mice **(Fig. 5d)**. In the central retina where Cre-induced degeneration was most prominent, we saw a significant increase in cell density of 34±10% after *E2F2* overexpression (P=0.0458). In the mid-periphery and periphery, smaller non-significant increases in cell density were observed.

RPE cells have an inherent capacity to proliferate. *In vitro*, mammalian RPE cells can be cultured for up to six months, undergoing several population doublings.[30] *In vivo*, RPE cells can proliferate as a natural reaction to disruption of the subretinal space during retinal detachment.[31-33] A necessary precondition for this kind of proliferation is disruption of cell-cell junctions to overcome contact inhibition. By *E2F2* gene transfer, we were able to induce proliferation *in situ,* without disruption of the RPE monolayer, and we showed that the biggest effect was achieved in the RPE area with the lowest cell density.

Subretinal injection itself is not free of trauma and might have induced some proliferation. However, injection of LNT-E2F2 vector caused limited BrdU uptake in cells evenly distributed throughout the injection area. Cells in the E2F2 treatment group showed variable cell size and

smaller cells gathered in clusters, potential signs of toxicity or the results of replication. If toxicity were the prevailing factor for altered morphology, we would expect dying cells to leave the monolayer and leaving gaps between cells. Since the RPE monolayer remained intact, we are confident that the cell morphology in the E2F2 treated RPE reflects the effects of cell division. BrdU uptake is a sign of DNA synthesis and therefore cell cycle progression from G1 to S phase, but this does not always signify completion of mitosis. We therefore focused on cell density as the main endpoint. To compensate for any effect of the injection trauma, we added untreated eyes that never received any subretinal injection as controls. Untreated eyes showed a slightly higher cell density compared with the controls injected with LNT-GFP or medium, possibly indicative of minor, injection-related cell loss, but this was not significant. The highest cell density was seen in the LNT-E2F2 treatment group, showing a significant increase of 14% compared with untreated RPE and 21% compared with control transduced RPE.

As for 9 week-old adult mice, we observed similar cell cycle progression in mice older than 18 months, which corresponds to a human age of >50 years, when age-related changes of the macula become apparent. However, mouse RPE does not show age-related changes comparable to human, and any extrapolation of our findings to patients with AMD calls for caution. Older human RPE cells in the central macula exposed to life-long oxidative stress may not be capable of undergoing a full cell division. Del Priore et al. found that the proportion of apoptotic cells in human RPE increased significantly with age, possibly amounting to a loss of 20% of the macular RPE per decade in older human eyes.[10] Interestingly, apoptosis was confined to the central region. In apparent contrast to Del Priore, Ach *et al.* showed that in the centre, human RPE cell density remains stable over lifetime.[34] This discrepancy may be explained by RPE undergoing a life-long re-arrangement, for example by migration from the periphery, possibly in combination with mitosis. In human adult RPE mitosis is detected at a very low rate, but only in the periphery.[10, 35] By *E2F2* transfer, we may be harnessing a natural process of mitotic regeneration that is latent in the adult mammalian retina. In the transgenic mouse model, which we utilize as a model for RPE cell disease, no spontaneous mitotic regeneration was detected, instead cells

expanded to up to 20 times their normal size, similar to what is observed in AMD patients.[32] Furthermore, we observe the presence of BrdU positive cells throughout the treatment area and the greatest proliferative effect of *E2F2* transfer in the centre where cell density was lowest. This indicates that the E2F2 triggers mitosis of cells *in situ* rather than recruiting cells from the periphery.

We and others have previously established that alterations made to the state of the cell cycle or cell-cell adhesion signalling pathways can result in de-differentiation of the RPE and the cells may undergo epithelial mesenchymal transition. This results in a dramatic loss of RPE cell identity both in terms of cell morphology and gene expression profile[36, 37]. Whilst transduced RPE (either by LNT-E2F2 or LNT-GFP) do display some morphological differences from untreated cells, the changes observed are much less severe than those seen in EMT in which cuboidal cell shape is lost. However, to examine whether any de-differentiation was occurring at the level of gene expression, we performed immunohistochemical staining for RPE65, a retinoid isomerohydrolase vital for RPE function. Transduction of the RPE with lentiviral vectors results in very sharp delineation of the transduced area. At 10 days post-injection the RPE65 signal was relatively homogenous across the boundary between the transduced and untransduced area in both LNT-E2F2 and LNT-GFP injected eyes, indicating little loss of RPE cell identity in transduced cells **(Fig 6).**

Whilst this study primarily focused upon the direct effect of E2F2 overexpression within the RPE, we also found no indication of an indirect effect upon the overlying photoreceptors, in terms of either structure or function within wildtype mice. It should be noted, however, that loss of vision in conditions such as AMD is thought to be a result of photoreceptor cell death as a consequence of RPE pathology. Any therapeutic strategy aiming to preserve or restore RPE integrity must therefore be applied prophylactically and the degree of photoreceptor degeneration will be critical in defining the treatment window.

Although no sign of neoplastic growth was seen over the timeframes used in these experiments, continuous E2F2 overexpression may lead to a tumorigenic event, as the protein in implicated in retinoblastoma and glioblastoma[38]. In these proof-of-concept experiments, we used non-integrating vectors resulting in episomal transgene copies, which will be diluted from the nucleus with every cell division. It is, however, possible that a temporary over-expression of E2F2, as we attempted here, could result in the establishment of a positive feedback loop that maintains the transduced cells within the cell cycle.[39] It may therefore be necessary to characterise more fully the effect of transient E2F2 overexpression upon the RPE cell cycle *in vivo* and implement additional safety measures. For example, an inducible promoter could be used to further control duration of expression, or a reverse transcriptase-defective lentiviral vector could be used, where reverse transcription of the transgene into DNA is prevented and the protein translated transiently from RNA templates.[40]

In summary, our work shows that viral vector mediated gene delivery of E2F2 can induce proliferation in healthy and diseased RPE cells *in vivo* and that this approach can increase cell density of RPE cells preferentially in areas of low density, where contact inhibition may be lowest. In mice, where assessments of vision are generally massed retinal responses, this localised rescue would not be sufficiently large to be able to detect improved vision. However, in the human eye, this approach may provide an alternative to RPE cell transplantation by paving the way for an *in situ* regenerative approach to treat RPE cell pathology in Stargardt disease and age-related macular degeneration (AMD).

Materials and Methods

Recombinant non-integrating lentiviral vectors

Self-inactivating VSV-G pseudotyped lentiviral vectors were produced using the packaging plasmid pCMVΔR8.74D64V as described previously.[41, 42] After transfection of HEK293T cells, vector particles were harvested from culture supernatant at 48 and 72 h post transfection and purified / concentrated by filtration (0.45 μm) and ultracentrifugation and suspended in serum-free OptiMEM at 10^7 to 10^8 transducing units/mL. See Supplementary Methods for details.

In vivo experiments

All animals were cared for in accordance with the UK Animal Scientific Procedures Act 1986 and procedures were in accordance with the ARVO Statement for the Use of Animals in Ophthalmic and Vision Research. Female wild-type C57BL6/J mice (Harlan Laboratories, Bicester, UK) were used aged 6-8 weeks or up to 18 months. In transgenic male and female RPE^{CreER}/DTA mice[11] RPE degeneration was induced by three intraperitoneal injections of 50μg tamoxifen during postnatal days 12–24. Transscleral subretinal injections were performed as previously described[43, 44], see Supplementary Methods. Per eye, two injections of 2 μl of viral suspension (5 x 10^7 vector particles/mL) were injected into the subretinal space. Group sizes were based on estimated variation and effect size. Animals and treatment eyes were not randomised.

Cell counts

Quantification of RPE cell density was done on confocal micrographs of masked samples by manually counting cells outlined with phalloidin or ZO-1 (using NIH ImageJ software, http://rsbweb.nih.gov/ij/, Version 1.46a). Masking was done on two levels: the flatmount slides were masked before imaging by an independent observer. Image acquisition and image analysis was done by different researchers, and the image labels were again masked. 6 micrographs per eye acquired in a standard pattern were counted and averaged.

Statistical analysis

Student's *t* test or analysis of variance tests were used as indicated for each experiment in the figure legends. Variance within groups was estimated to determine similarity between groups being compared. $P<0.05$ was deemed significant.

Acknowledgments

This work was supported by the National Institute for Health Research Biomedical Research Centre at Moorfields Eye Hospital and UCL and also by Moorfields Eye Charity. The authors gratefully acknowledge Anselm Kampik, Augenzentrum im Brienner Hof, Munich, Germany, for helpful discussions. The authors thank Nancy Joyce, Schepens Eye Research Institute, Harvard Medical School, Boston, USA, for providing the human *E2F2* cDNA plasmid.

Conflict of interest

U.F.O. Luhmann is employee of F. Hoffmann-La Roche Ltd. All other authors declare that no competing financial interests exist.

Supplementary information is available at Gene Therapy's website

Reference List

(1) Gehrs KM, Anderson DH, Johnson LV, Hageman GS. Age-related macular degeneration--emerging pathogenetic and therapeutic concepts. *Ann Med* 2006; 38: 450-471.

(2) Klein R, Klein BE, Jensen SC, Meuer SM. The five-year incidence and progression of age-related maculopathy: the Beaver Dam Eye Study. *Ophthalmology* 1997; 104: 7-21.

(3) Klein R, Klein BE, Linton KL. Prevalence of age-related maculopathy. The Beaver Dam Eye Study. *Ophthalmology* 1992; 99: 933-943.

(4) Friedman DS, O'Colmain BJ, Munoz B, Tomany SC, McCarty C, de Jong PT, et al. Prevalence of age-related macular degeneration in the United States. *Arch Ophthalmol* 2004; 122: 564-572.

(5) Strauss O. The retinal pigment epithelium in visual function. *Physiol Rev* 2005; 85: 845-881.

(6) Ambati J, Ambati BK, Yoo SH, Ianchulev S, Adamis AP. Age-related macular degeneration: etiology, pathogenesis, and therapeutic strategies. *Surv Ophthalmol* 2003; 48: 257-293.

(7) Dorey CK, Wu G, Ebenstein D, Garsd A, Weiter JJ. Cell loss in the aging retina. Relationship to lipofuscin accumulation and macular degeneration. *Invest Ophthalmol Vis Sci* 1989; 30: 1691-1699.

(8) Marshall J. The ageing retina: physiology or pathology. *Eye (Lond)* 1987; 1 (Pt 2): 282-295.

(9) Kaldarar-Pedotti S. [Mitotic activity of the pigment epithelium during embryonic and postembryonic development]. *Adv Ophthalmol* 1979; 39: 37-58.

(10) Del Priore LV, Kuo YH, Tezel TH. Age-related changes in human RPE cell density and apoptosis proportion in situ. *Invest Ophthalmol Vis Sci* 2002; 43: 3312-3318.

(11) Longbottom R, Fruttiger M, Douglas RH, Martinez-Barbera JP, Greenwood J, Moss SE. Genetic ablation of retinal pigment epithelial cells reveals the adaptive response of the epithelium and impact on photoreceptors. *Proc Natl Acad Sci U S A* 2009; 106: 18728-18733.

(12) Machemer R, Steinhorst UH. Retinal separation, retinotomy, and macular relocation: II. A surgical approach for age-related macular degeneration? *Graefes Arch Clin Exp Ophthalmol* 1993; 231: 635-641.

(13) Eandi CM, Giansanti F, Virgili G. Macular translocation for neovascular age-related macular degeneration. *Cochrane Database Syst Rev* 2008; CD006928.

(14) MacLaren RE, Bird AC, Sathia PJ, Aylward GW. Long-term results of submacular surgery combined with macular translocation of the retinal pigment epithelium in neovascular age-related macular degeneration. *Ophthalmology* 2005; 112: 2081-2087.

(15) da CL, Chen FK, Ahmado A, Greenwood J, Coffey P. RPE transplantation and its role in retinal disease. *Prog Retin Eye Res* 2007; 26: 598-635.

(16) Binder S, Stanzel BV, Krebs I, Glittenberg C. Transplantation of the RPE in AMD. *Prog Retin Eye Res* 2007; 26: 516-554.

(17) van Romunde SH, Polito A, Bertazzi L, Guerriero M, Pertile G. Long-Term Results of Full Macular Translocation for Choroidal Neovascularization in Age-Related Macular Degeneration. *Ophthalmology* 2015; 122: 1366-1374.

(18) Aisenbrey S, Lafaut BA, Szurman P, Hilgers RD, Esser P, Walter P, et al. Iris pigment epithelial translocation in the treatment of exudative macular degeneration: a 3-year follow-up. *Arch Ophthalmol* 2006; 124: 183-188.

(19) Joussen AM, Joeres S, Fawzy N, Heussen FM, Llacer H, van Meurs JC, et al. Autologous translocation of the choroid and retinal pigment epithelium in patients with geographic atrophy. *Ophthalmology* 2007; 114: 551-560.

(20) MacLaren RE, Uppal GS, Balaggan KS, Tufail A, Munro PM, Milliken AB, et al. Autologous transplantation of the retinal pigment epithelium and choroid in the treatment of neovascular age-related macular degeneration. *Ophthalmology* 2007; 114: 561-570.

(21) van Meurs JC, ter AE, Croxen R, Hofland L, van Hagen PM. Comparison of the growth potential of retinal pigment epithelial cells obtained during vitrectomy in patients with age-related macular degeneration or complex retinal detachment. *Graefes Arch Clin Exp Ophthalmol* 2004; 242: 442-443.

(22) Gouras P, Flood MT, Kjedbye H, Bilek MK, Eggers H. Transplantation of cultured human retinal epithelium to Bruch's membrane of the owl monkey's eye. *Curr Eye Res* 1985; 4: 253-265.

(23) Schwartz SD, Regillo CD, Lam BL, Eliott D, Rosenfeld PJ, Gregori NZ, et al. Human embryonic stem cell-derived retinal pigment epithelium in patients with age-related macular degeneration and Stargardt's macular dystrophy: follow-up of two open-label phase 1/2 studies. *Lancet* 2015; 385: 509-516.

(24) Cyranoski D. Stem cells cruise to clinic. *Nature* 2013; 494: 413.

(25) Song P, Inagaki Y, Sugawara Y, Kokudo N. Perspectives on human clinical trials of therapies using iPS cells in Japan: reaching the forefront of stem-cell therapies. *Biosci Trends* 2013; 7: 157-158.

(26) Dyson N. The regulation of E2F by pRB-family proteins. *Genes Dev* 1998; 12: 2245-2262.

(27) Nevins JR. The Rb/E2F pathway and cancer. *Hum Mol Genet* 2001; 10: 699-703.

(28) Wu L, Timmers C, Maiti B, Saavedra HI, Sang L, Chong GT, et al. The E2F1-3 transcription factors are essential for cellular proliferation. *Nature* 2001; 414: 457-462.

(29) DeGregori J, Leone G, Miron A, Jakoi L, Nevins JR. Distinct roles for E2F proteins in cell growth control and apoptosis. *Proc Natl Acad Sci U S A* 1997; 94: 7245-7250.

(30) Albert DM, Tso MO, Rabson AS. In vitro growth of pure cultures of retinal pigment epithelium. *Arch Ophthalmol* 1972; 88: 63-69.

(31) Machemer R, Laqua H. Pigment epithelium proliferation in retinal detachment (massive periretinal proliferation). *Am J Ophthalmol* 1975; 80: 1-23.

(32) Machemer R, van HD, Aaberg TM. Pigment epithelial proliferation in human retinal detachment with massive periretinal proliferation. *Am J Ophthalmol* 1978; 85: 181-191.

(33) Anderson DH, Stern WH, Fisher SK, Erickson PA, Borgula GA. The onset of pigment epithelial proliferation after retinal detachment. *Invest Ophthalmol Vis Sci* 1981; 21: 10-16.

(34) Ach T, Huisingh C, McGwin G, Jr., Messinger JD, Zhang T, Bentley MJ, et al. Quantitative autofluorescence and cell density maps of the human retinal pigment epithelium. *Invest Ophthalmol Vis Sci* 2014; 55: 4832-4841.

(35) Al-Hussaini H, Kam JH, Vugler A, Semo M, Jeffery G. Mature retinal pigment epithelium cells are retained in the cell cycle and proliferate in vivo. *Mol Vis* 2008; 14: 1784-1791.

(36) Georgiadis A, Tschernutter M, Bainbridge JW, Balaggan KS, Mowat F, West EL, et al. The tight junction associated signalling proteins ZO-1 and ZONAB regulate retinal pigment epithelium homeostasis in mice. *PLoS One* 2010; 5: e15730.

(37) Tamiya S, Liu L, Kaplan HJ. Epithelial-mesenchymal transition and proliferation of retinal pigment epithelial cells initiated upon loss of cell-cell contact. *Invest Ophthalmol Vis Sci* 2010; 51: 2755-2763.

(38) Bracken AP, Ciro M, Cocito A, Helin K. E2F target genes: unraveling the biology. *Trends Biochem Sci* 2004; 29: 409-417.

(39) Jirawatnotai S, Sharma S, Michowski W, Suktitipat B, Geng Y, Quackenbush J, et al. The cyclin D1-CDK4 oncogenic interactome enables identification of potential novel oncogenes and clinical prognosis. *Cell Cycle* 2014; 13: 2889-2900.

(40) Galla M, Schambach A, Towers GJ, Baum C. Cellular restriction of retrovirus particle-mediated mRNA transfer. *J Virol* 2008; 82: 3069-3077.

(41) Demaison C, Parsley K, Brouns G, Scherr M, Battmer K, Kinnon C, et al. High-level transduction and gene expression in hematopoietic repopulating cells using a human immunodeficiency [correction of imunodeficiency] virus type 1-based lentiviral vector containing an internal spleen focus forming virus promoter. *Hum Gene Ther* 2002; 13: 803-813.

(42) Yanez-Munoz RJ, Balaggan KS, MacNeil A, Howe SJ, Schmidt M, Smith AJ, et al. Effective gene therapy with nonintegrating lentiviral vectors. *Nat Med* 2006; 12: 348-353.

(43) Bainbridge JWB, Stephens C, Parsley K, Demaison C, Halfyard A, Thrasher AJ, et al. In vivo gene transfer to the mouse eye using an HIV-based lentiviral vector; efficient long-term transduction of corneal endothelium and retinal pigment epithelium. *Gene Ther* 2001; 8: 1665-1668.

(44) Ali RR, Reichel MB, Thrasher AJ, Levinsky RJ, Kinnon C, Kanuga N, et al. Gene transfer into the mouse retina mediated by an adeno-associated viral vector. *Hum Mol Genet* 1996; 5: 591-594.

444

445

446 Figure legends

447

448 **Fig. 1. *E2F2* overexpression induces proliferation in a growth arrested, confluent monolayer of**
449 **ARPE19 cells *in vitro*.**

450 a. 21 days post-transfection with pCMVHA-E2F2, *E2F2* mRNA is >1000-fold increased compared
451 with controls transfected with pcDNA3-EGFP (mean + SD).

452 b, c. Increase in protein levels of E2F2 compared with control, assessed by Western blot (9-fold
453 increase after 2 days, 3-fold increase after 7 days; 2-tailed *t*-test; densidometric quantification, 5
454 min and 30 min indicate different exposure times, mean + SD).

455 b, d. Levels of proliferation marker Cyclin D1 increased following *E2F2* overexpression (2- and
456 3-fold, on day 2 and 7, respectively).

457 e. *E2F2* overexpression induces *Ki67* expression. On day 7 and 14 post transfection, E2F2
458 caused a 2.3-fold and 1.7-fold increase in Ki67 positive nuclei compared with controls (40% vs.
459 18% and 7% vs. 4% of total cells; 2-tailed *t*-test).

460 f. *E2F2* overexpression induces BrdU uptake. BrdU positive nuclei were increased by 3.5- and
461 5.4-fold at 1 and 2 weeks post transfection, respectively (2-tailed *t*-test).

462

463

Fig. 2. LNT-E2F2 induces BrdU uptake in RPE *in vivo.*

Wildtype mice received daily intraperitoneal injections of BrdU from day 4 to day 10 after subretinal injections of vector (n=4 eyes per group from different animals).

a. RPE-choroid-sclera was immunostained for E2F2 (green) and BrdU (red) and flatmounted for imaging on a confocal laser scanning microscope. Analysis included injected areas, identified by a demarcation line along the border of the former injection bleb, clearly visible on flatmounts (outlined by arrowheads), but excluded the injection site with trauma-related artefacts (arrow). Scale bar = 1mm.

b. In LNT-E2F2 injected eyes, RPE flat mounts show overexpression of E2F2 co-localizing with BrdU. Controls show very limited staining for E2F2 (medium) or BrdU (medium, LNT-GFP). Scale bar = 75 µm.

c, d. Counts of E2F2 positive nuclei were correlated with counts of BrdU positive nuclei for each high power microscopic field (HPF, total of 20 HPFs, 5 per eye). In the LNT-E2F2 group, a high linear correlation was observed (Pearson correlation coefficient 0.9170, r^2=0.841, P<0.0001), while no correlation was observed for the medium injected control group.

e. The LNT-E2F2 injected group showed a significant increase in E2F2 and BrdU staining compared with both control groups (mice aged 9 weeks, n=4 eyes per group from different animals, P<0.0001, one-way ANOVA; *** P<0.0001 in Tukey's multiple comparisons test, no significant difference between both control groups; bars represent mean ± SD). E2F2 and BrdU positive nuclei were counted in 5 HPF per eye and averaged.

f. 18 months old mice (n=3 mice for pairwise left-right comparison) demonstrate a similar increase in BrdU uptake upon *E2F2* overexpression (* P=0.0463, 2-tailed paired *t*-test; bars represent mean ± SD).

Fig. 3. *E2F2* overexpression increases RPE cell density *in vivo*.

a. Immunofluorescence staining of f-actin of flatmounted RPE shows cell outlines of the RPE monolayer. *E2F2* overexpression in the treatment group was verified by immunostaining. Scale bar = 100 μm.

b. Quantification of RPE cell density was done on masked samples by counting cells. 6 micrographs per eye were counted and averaged, for each condition n=15 eyes from different animals, for medium controls n=8. Numbers in graph represent mean cell density; error bars represent SD. One-way ANOVA revealed highly significant differences among groups (P=0.0002). LNT-E2F2 treatment increased cell density by 17 ±13% compared to LNT-GFP, by 21 ±14% compared to medium injection, and by 14 ±7% compared to untreated eyes (Tukey's multiple comparisons test).

Fig. 4. The RPE^{CreER}/DTA mouse line shows reduced RPE cell density most prominently in the centre.

a. ZO-1 staining reveals increased cell size and polymorphism in the RPE ablated group in various locations along the central to peripheral axis. Scale bar = 50 μm.

b. Overall density was reduced by 15 ±5% (mean ± SEM, range 5 – 25%, values in graph above the x axis are mean ±SD, n=8 eyes per group, P=0.0082, 2-tailed t-test).

c. Reduction was most pronounced in the central RPE, showing a 24 ±10% decrease (mean +SEM, n=8 eyes, P=0.0231, 2-tailed unpaired t-test).

Fig. 5. LNT-E2F2 induces increased BrdU uptake in RPE^{CreER}/DTA mice and increases RPE cell density.

a. Schematic representation of the RPE flatmounts to illustrate regional analysis of cell density.

b. Treatment vector LNT-E2F2 and control vector LNT-GFP were injected in right and left eyes, respectively, of RPE^{CreER}/DTA mice (n=4 eyes per group). Mice received daily intraperitoneal BrdU injections on day 3 to 9 post injection. BrdU staining (red) is shown in representative RPE flatmounts. Scale bar = 500 µm.

c. Quantification of BrdU positive nuclei in 6 micrographs per flatmount revealed a significant increase compared to LNT-GFP treated controls (P=0.0173, 2-tailed paired t-test, n=4 eyes per group, bars show mean ± SEM).

d. Regional analysis of cell density shows a statistically significant increase in the centre where RPE degeneration was strongest. Here, an average increase of 34 ±10% was observed (P=0.0458, 2-tailed paired t-test, n=4 eyes per group, bars show mean +SEM).

Fig. 6. Lentivirus-mediated overexpression of E2F2 does not lead to dedifferentiation of RPE cells, as evidenced by the presence of RPE65

Staining for RPE-specific protein RPE65 in RPE flatmounts 10 days after subretinal administration of LNT-E2F2 showed no consistent decrease in cells positive for E2F2 protein in the nucleus, compared with E2F2 negative cells. RPE transduced with LNT-GFP control virus and no-primary control samples are provided as controls. Scale bar = 50 µm

Supplementary Material

Fig. S1. Growth arrest in ARPE19 cells.

a. ARPE19 cells were cultured in starvation medium containing 1 % FBS. Over the course of 2–3 weeks, expression of tight junction marker ZO-1 (green) increased while the proportion of cells positive for proliferation marker Ki67 (red) decreased. Scale bar = 100 µm.

b. The proportion of Ki67 positive cells showed inverse correlation to the total number of cells, indicating growth arrest.

Fig. S2. LNT-E2F2 induces BrdU uptake in RPE *in vivo*.

Wildtype mice aged 12 weeks received subretinal injections of non-integrating LNT-E2F2 vector (2 x 10^5 infectious particles per eye) in the superior and inferior hemisphere of the eye. Titre matched LNT-hrGFP and medium (OptiMEM) injected eyes served as controls (n=3 eyes per group from different animals). All mice received daily intraperitoneal injections of BrdU from day 4 onwards until they were sacrificed 8 days post injection.

a. RPE-choroid-sclera was immunostained for E2F2 and BrdU and flatmounted for imaging on a confocal laser scanning microscope. Analysis included injected areas only, injection sites with trauma-related artefacts were excluded. In LNT-E2F2 injected eyes, RPE flat mounts show overexpression of E2F2 co-localizing with BrdU. Controls show very limited staining for E2F2 (medium) or BrdU (medium, LNT-GFP). Scale bar = 250 µm.

b. The LNT-E2F2 injected group showed a significant increase of E2F2 and BrdU staining compared to both control groups ($P<0.0005$, one-way ANOVA; ** $P<0.005$, *** $P<0.0005$ in Tukey's multiple comparisons test, no significant difference between both control groups; bars represent mean ± SD). E2F2 and BrdU positive nuclei were counted in 5 high power microscopic fields (HPF) per eye and averaged.

Fig. S3. LNT-E2F2 does not affect photoreceptor function and histology.

Wildtype mice aged 8 weeks received subretinal injections of non-integrating LNT-E2F2 vector (2 x 10^5 infectious particles per eye) in the superior and inferior hemisphere of the eye. Titre matched LNT-GFP and uninjected eyes served as controls (n=8 eyes per group from different animals).

a. Photopic [10cd.s/m^2] ERG b-wave amplitudes in LNT-E2F2 and LNT-GFP injected eyes at 10 and 30 days post injection (DPI). Uninjected control also shown for reference. No significant differences were found (One-way ANOVA with Tukeys multiple comparisons test).

b. Scotopic [0.01cd.s/m2] ERG b-wave amplitudes in LNT-E2F2 and LNT-GFP injected eyes at 10 and 30 days post injection (DPI). Uninjected control also shown for reference. No significant differences were found (One-way ANOVA with Tukeys multiple comparisons test).

c. Representative retinal histology of LNT-E2F2 and LNT-GFP injected eyes at 10 and 30 days post injection (DPI). All images taken from the mid superior retina ~600μM from the optic nerve head. Scale bar = 100 μM.

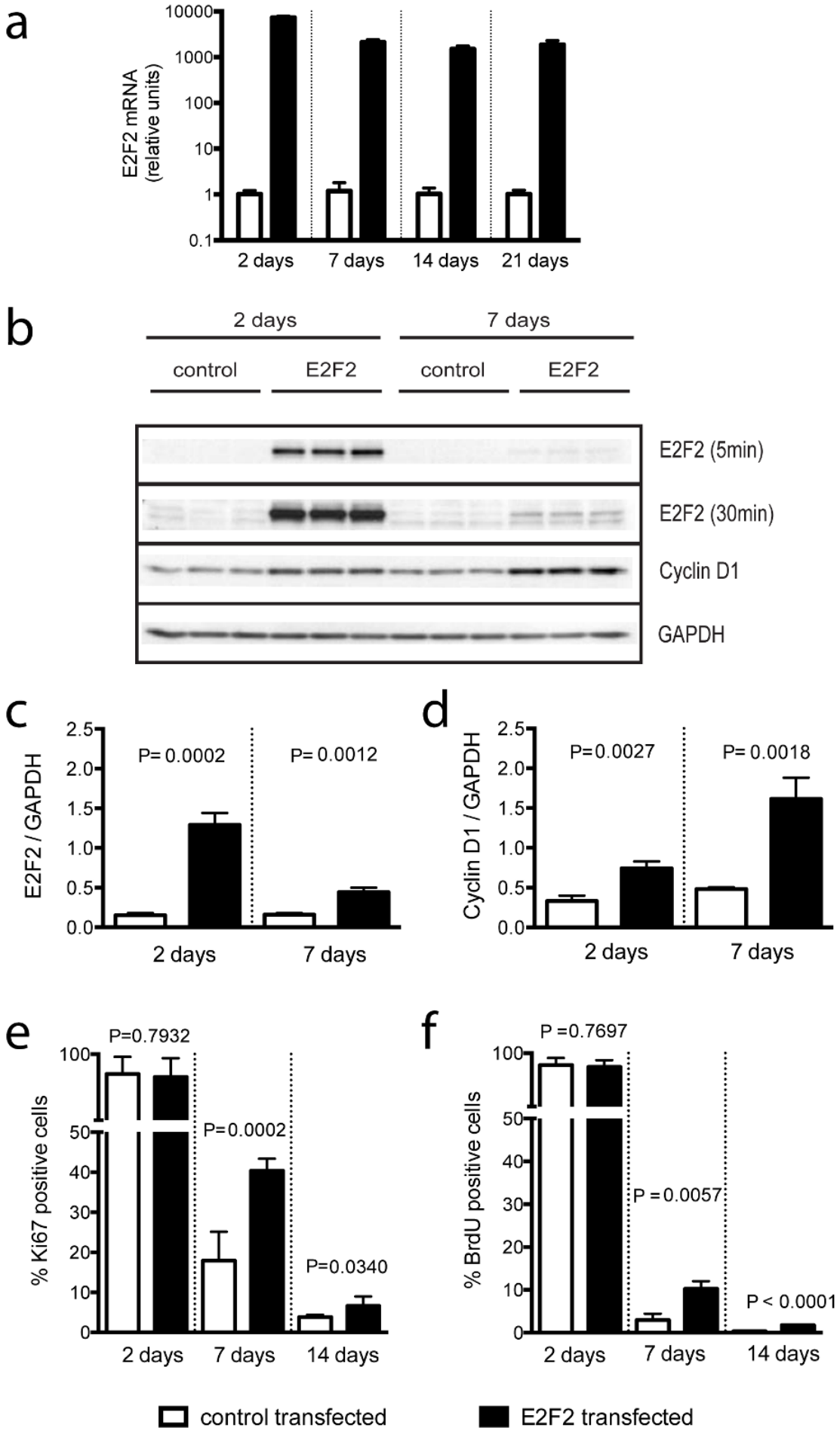
a
E2F2 mRNA (relative units)
10000
1000
100
10
1
0.1
2 days
7 days
14 days
21 days
b
2 days
7 days
control
E2F2
control
E2F2
E2F2 (5min)
E2F2 (30min)
Cyclin D1
GAPDH
c
E2F2 / GAPDH
P= 0.0002
P= 0.0012
2 days
7 days
d
Cyclin D1 / GAPDH
P=0.0027
P= 0.0018
2 days
7 days
e
% Ki67 positive cells
P=0.7932
P=0.0002
P=0.0340
2 days
7 days
14 days
f
% BrdU positive cells
P =0.7697
P = 0.0057
P < 0.0001
2 days
7 days
14 days
control transfected
E2F2 transfected

Figure 1

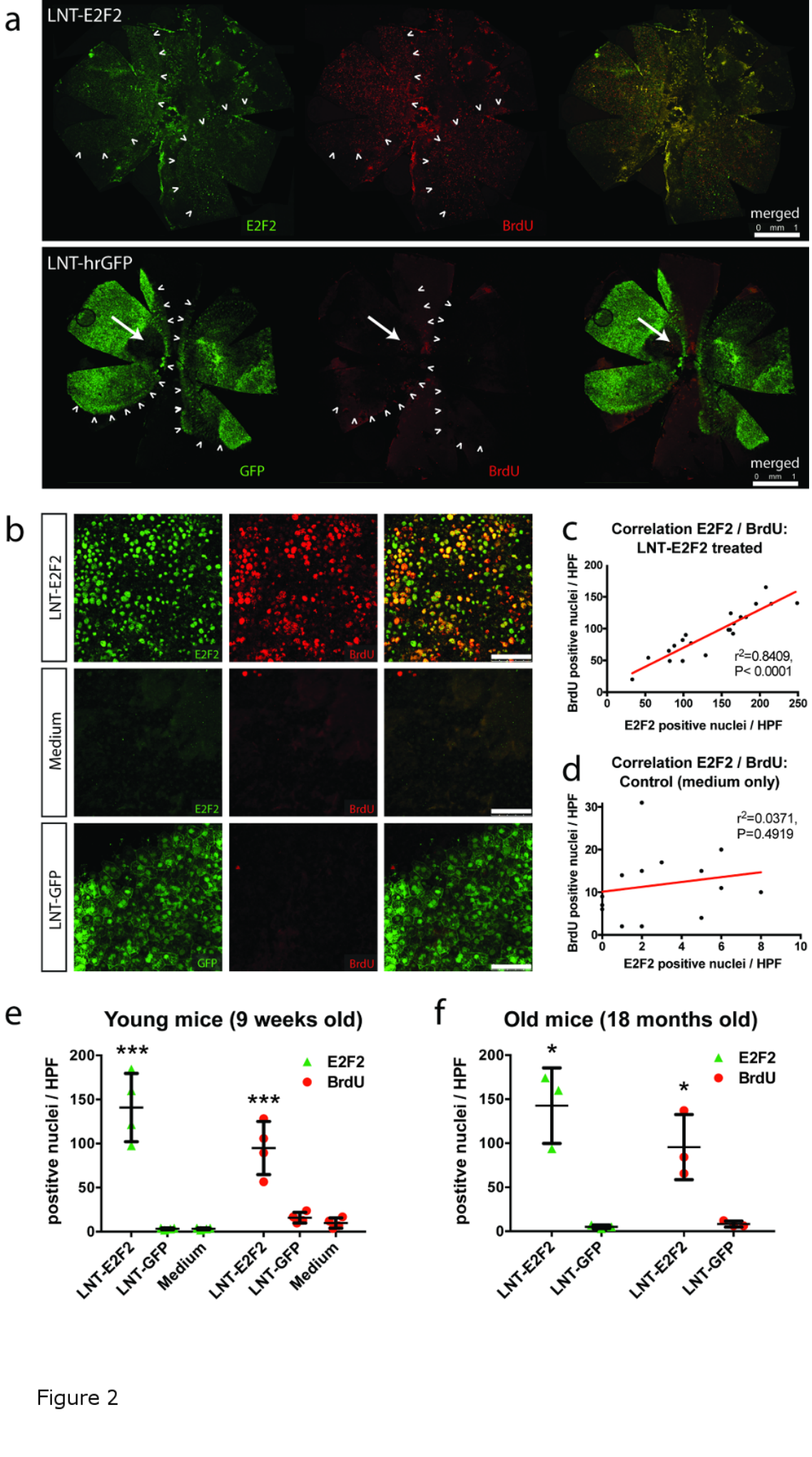
a
LNT-E2F2
E2F2
BrdU
merged
LNT-hrGFP
GFP
BrdU
merged
b
LNT-E2F2
Medium
LNT-GFP
E2F2
BrdU
GFP
BrdU
c
Correlation E2F2 / BrdU:
LNT-E2F2 treated
BrdU positive nuclei / HPF
E2F2 positive nuclei / HPF
r²=0.8409,
P< 0.0001
d
Correlation E2F2 / BrdU:
Control (medium only)
BrdU positive nuclei / HPF
E2F2 positive nuclei / HPF
r²=0.0371,
P=0.4919
e
Young mice (9 weeks old)
postitve nuclei / HPF
E2F2
BrdU
***
***
LNT-E2F2
LNT-GFP
Medium
LNT-E2F2
LNT-GFP
Medium
f
Old mice (18 months old)
postitve nuclei / HPF
E2F2
BrdU
*
*
LNT-E2F2
LNT-GFP
LNT-E2F2
LNT-GFP

Figure 2

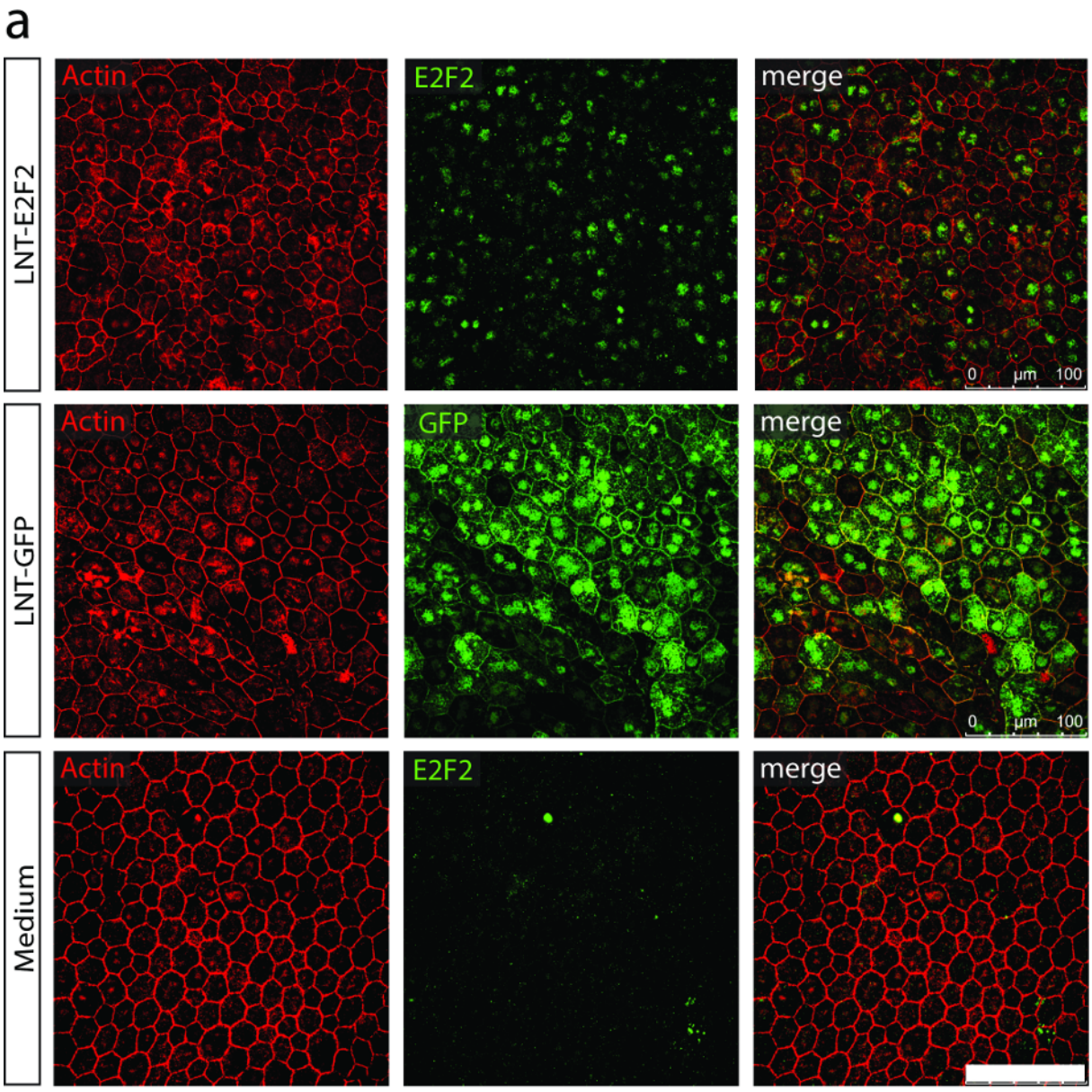
a
LNT-E2F2
Actin
E2F2
merge
0 µm 100
LNT-GFP
Actin
GFP
merge
0 µm 100
Medium
Actin
E2F2
merge
b
P=0.0011
P=0.0011
P=0.0071
cells per mm2
4000
3000
2000
1000
0
2961
±317
2534
±318
2449
±354
2600
±176
LNT-E2F2
LNT-GFP
Medium
Untreated

Figure 3

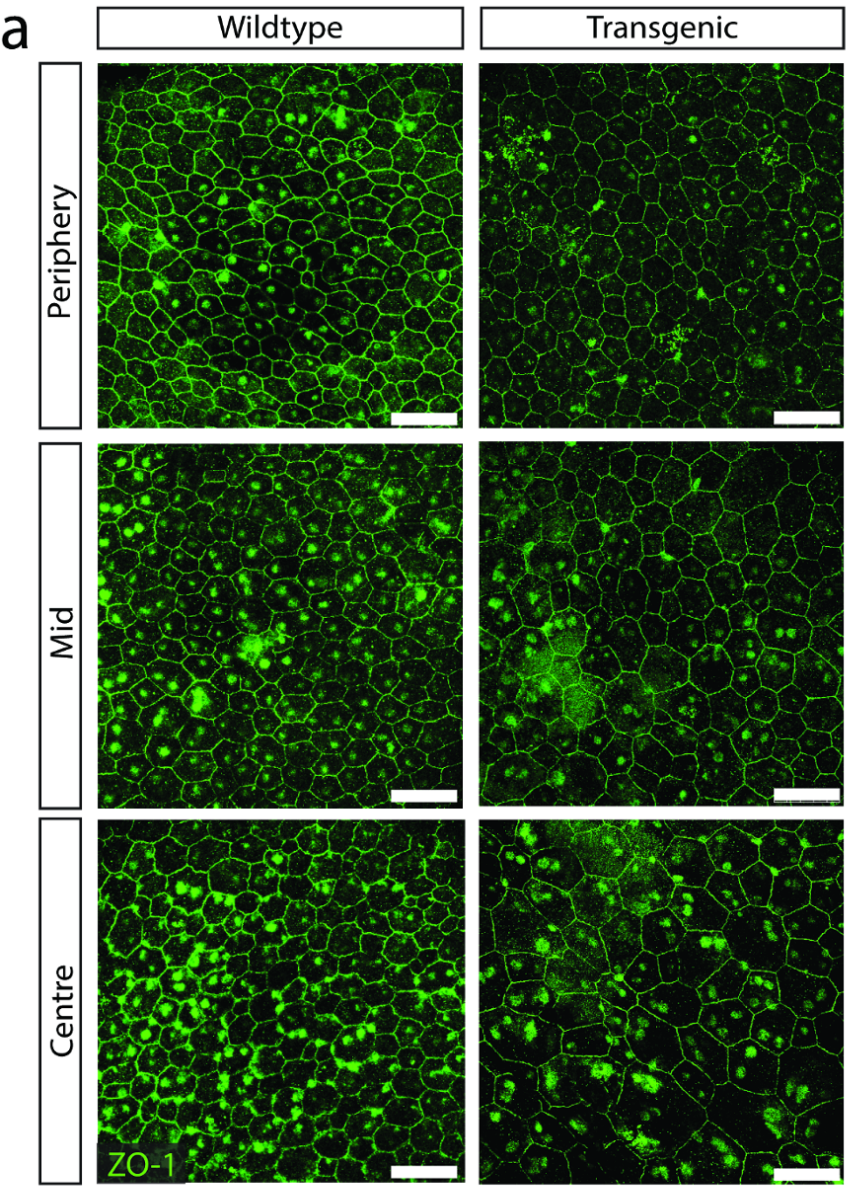
a
Wildtype
Transgenic
Periphery
Mid
Centre
ZO-1

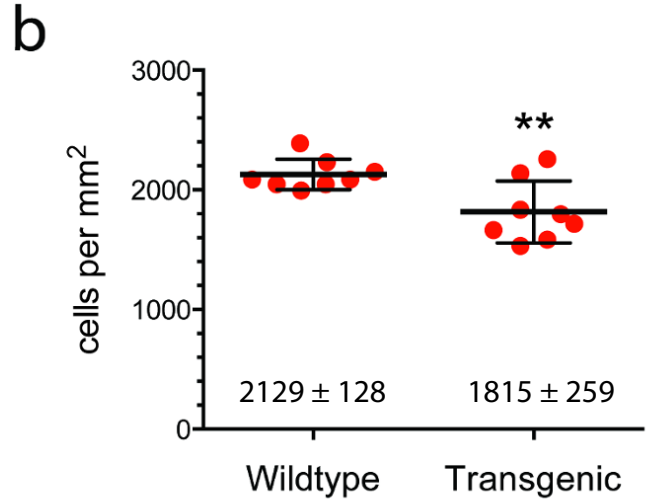
b
3000
2000
1000
0
cells per mm2
**
2129 ± 128
1815 ± 259
Wildtype
Transgenic

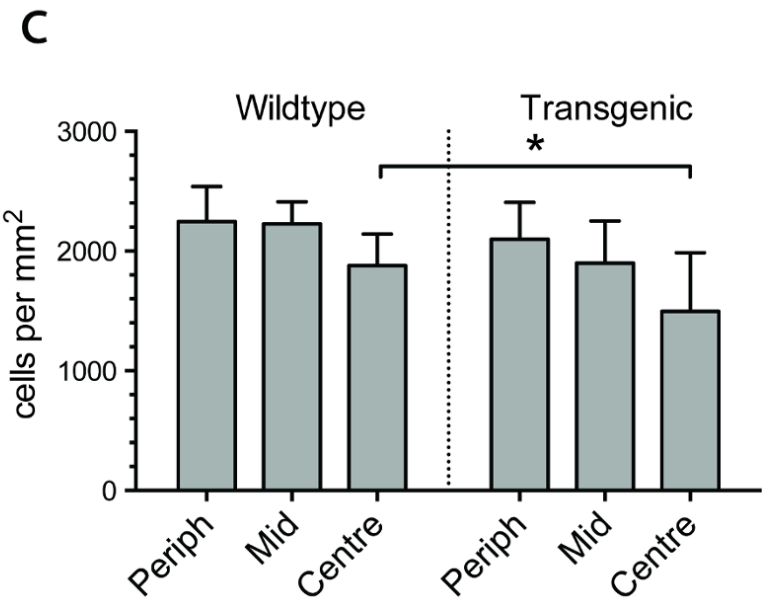
c
Wildtype
Transgenic
*
3000
2000
1000
0
cells per mm2
Periph
Mid
Centre
Periph
Mid
Centre

Figure 4

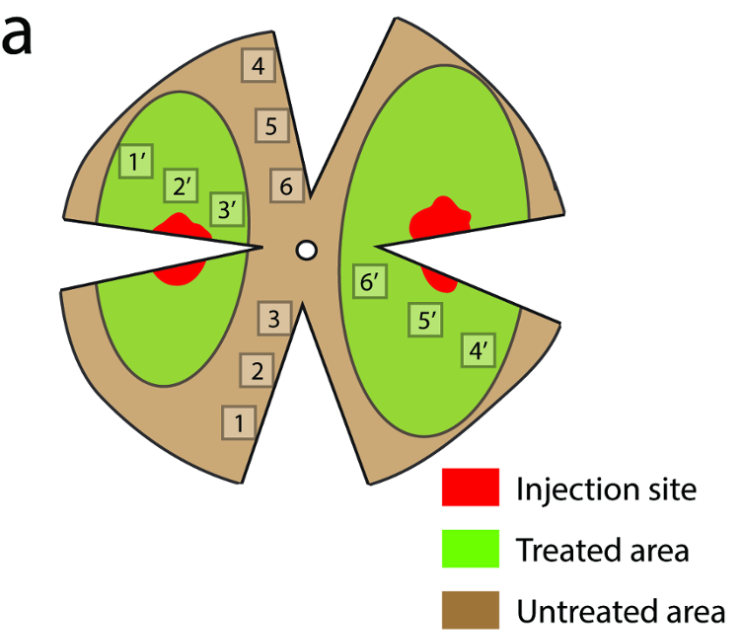
a
4
5
1′
2′
3′
6
6′
5′
4′
3
2
1
Injection site
Treated area
Untreated area

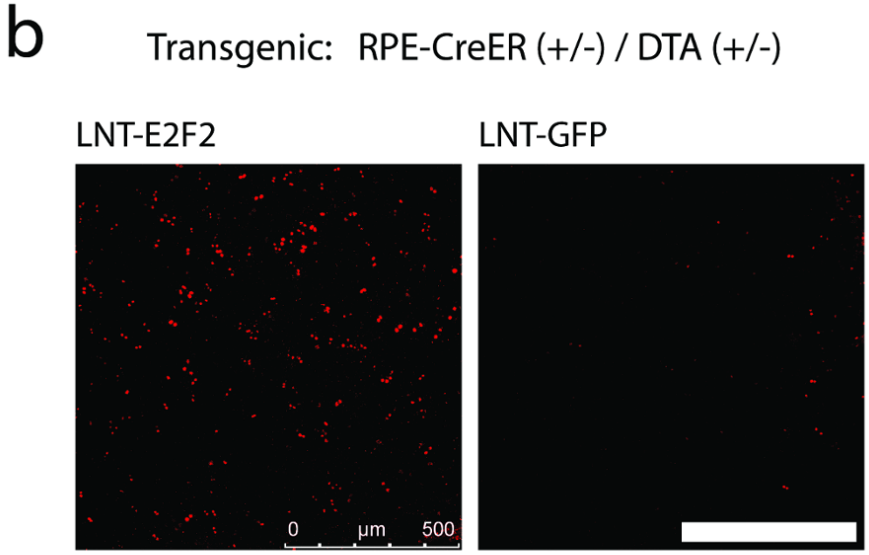
b
Transgenic: RPE-CreER (+/-) / DTA (+/-)
LNT-E2F2
LNT-GFP
0
µm
500

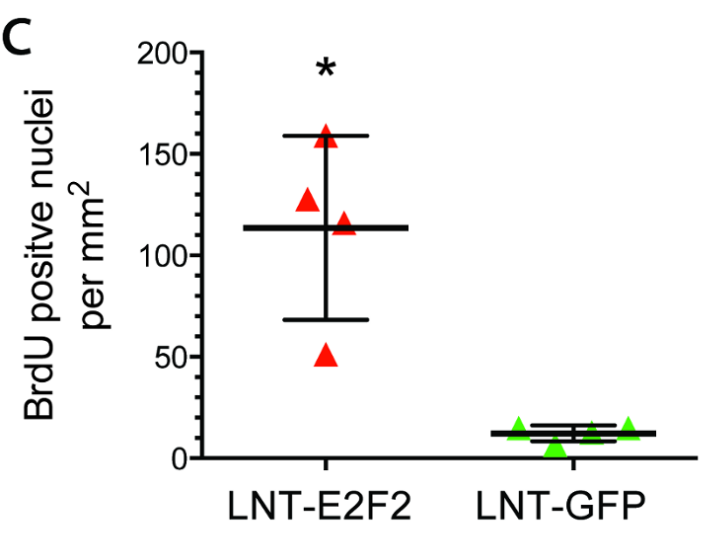
c
BrdU positve nuclei per mm2
200
150
100
50
0
*
LNT-E2F2
LNT-GFP

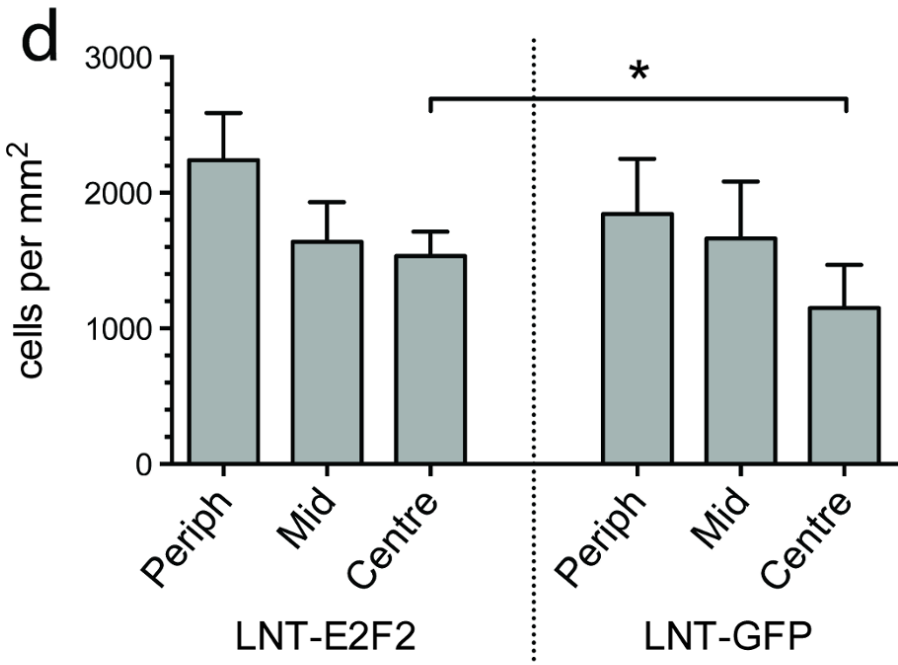
d
cells per mm2
3000
2000
1000
0
*
Periph
Mid
Centre
Periph
Mid
Centre
LNT-E2F2
LNT-GFP

Figure 5

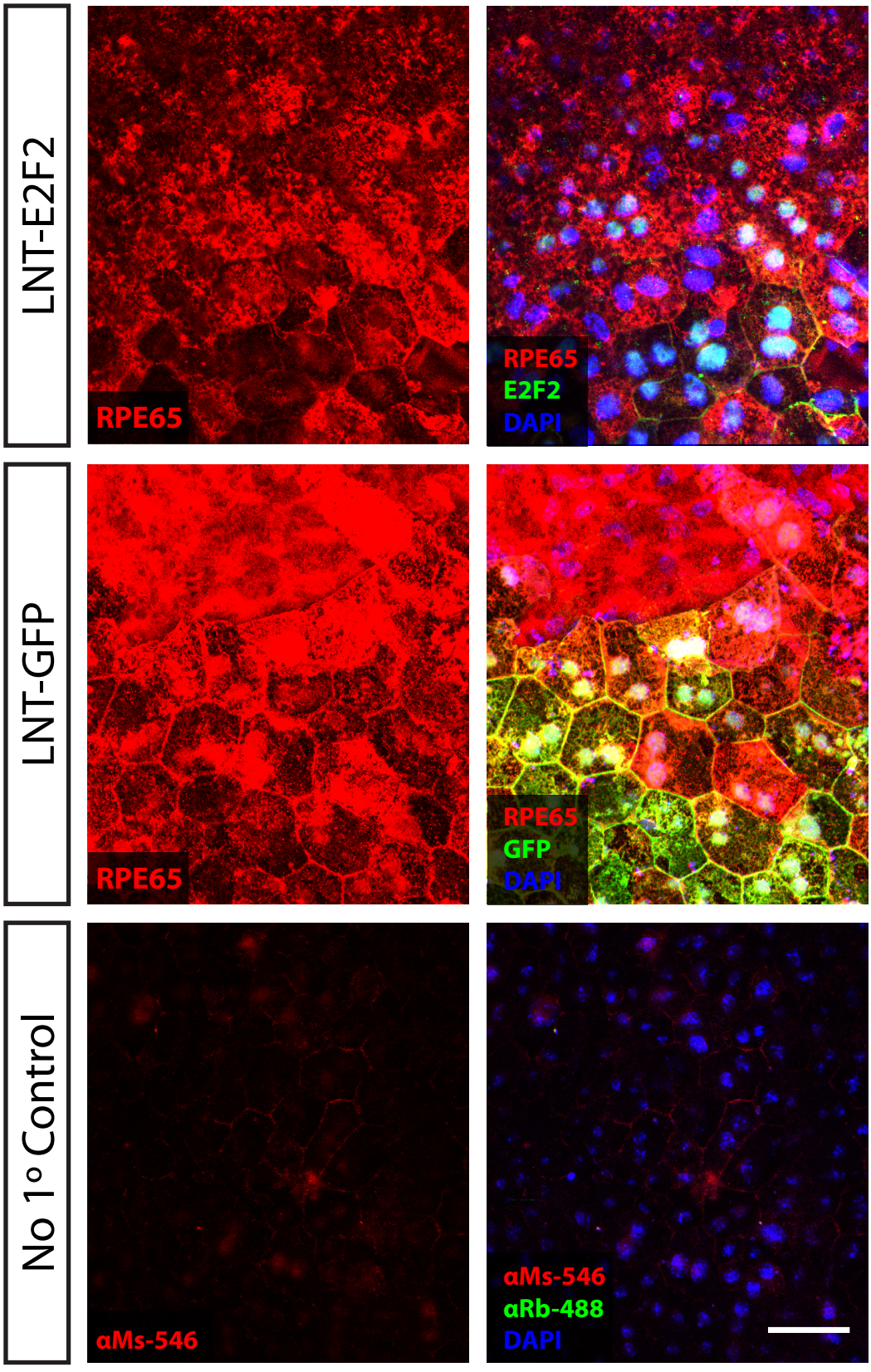
LNT-E2F2
RPE65
RPE65
E2F2
DAPI
LNT-GFP
RPE65
RPE65
GFP
DAPI
No 1° Control
αMs-546
αMs-546
αRb-488
DAPI

Supplementary Methods

Recombinant non-integrating lentiviral vectors

Self-inactivating VSV-G pseudotyped lentiviral vectors were produced as described previously[1] using the following plasmids: packaging plasmid pCMVΔR8.74D64V,[2] envelope plasmid pMD2.G,[3] and transfer vector based on pHR'SIN-cPPT.[4] Plasmids were prepared at a molar ratio of 50 : 17.5 : 32.5, and 80 µg of total plasmid DNA per 150 cm^2 culture dish was used for transient transfection of near-confluent HEK-293T cells using PEI. Vector particles were harvested from culture supernatant at 48 and 72 h post transfection and purified / concentrated by filtration (0.45 µm) and ultracentrifugation. Vector particles were suspended in serum-free OptiMEM (Life Technologies, Paisley, UK), which was also used for control medium-only subretinal injections. Vector titres were determined by transduction of 293T cells with serial vector dilutions (LNT-GFP) or by quantification of reverse transcriptase using the Reverse Transcriptase Assay colorimetric kit (Roche). Vector concentration was 10^7 to 10^8 transducing units/mL.

For *E2F2* cDNA transduction, *E2F2* was inserted into the transfer plasmid behind the CMV promoter by restriction enzyme digestion and directional ligation. The resulting vector was named LNT-E2F2. Human full-length *E2F2* cDNA (1313 bp) was derived from plasmid pCMV-E2F2, kindly provided by Dr Nancy Joyce, Schepens Eye Research Institute, Harvard Medical School, Boston, USA.[5, 6] LNT-GFP, based on the same production plasmids, was used as control vector delivering *hrGFP*.[7]

In vitro experiments

ARPE19 cells (ATCC CRL-2302, Manassas, VA) were cultured in DMEM/F12 containing 100 U/mL penicillin and 100 µg/mL streptomycin (all from PAA Laboratories, Pasching, Austria) and 10% fetal bovine serum (FBS, Biochrom, Berlin, Germany). Cells were seeded in equal densities to 24 well plates and after 24 hours, medium was changed to 1% FBS. After 2 weeks

with medium exchange twice a week, a confluent monolayer with ZO-1 positive cell borders and no mitotic activity was formed (cf. Fig. S1). At this stage, cells were used for transfection using linear polyethylenimine (PEI, Polysciences, Eppelheim, Germany) pre-incubated with plasmid at a ratio of 2.25 : 1 (w/w) for 20 min and added to cells for 24 h. Plasmids were obtained from Addgene, Cambridge, MA: pCMVHA-E2F2 (plasmid #24226, delivering *E2F2* under CMV promoter)[8], pcDNA3-EGFP (#13031, delivering eGFP under CMV promoter), pCMV-Neo-Bam (#16440, empty plasmid).

In vivo experiments

All animals were cared for in accordance with the UK Animal Scientific Procedures Act 1986 and procedures were in accordance with the ARVO Statement for the Use of Animals in Ophthalmic and Vision Research. Female wild-type C57BL6/J mice (Harlan Laboratories, Bicester, UK) were used aged 6-8 weeks or up to 18 months. In transgenic male and female RPE^{CreER}/DTA mice,[9] RPE degeneration was induced by three intraperitoneal injections of 50µg tamoxifen during postnatal days 12–24.

Animals were anaesthetised with intraperitoneal injection of medetomidine hydrochloride (1 mg/ml, Domitor, Pfizer Pharmaceuticals, Walton Oaks, UK) and ketamine (100 mg/ml, Fort Dodge Animal Health, Southampton, UK) and sterile water in the ratio 5:3:42. Transscleral subretinal injections were performed as previously described[4, 10] under direct vision of the fundus with an operating microscope. Per eye, two injections of 2 µl of viral suspension (5×10^7 vector particles/mL) were injected into the subretinal space causing a localised retinal detachment. For BrdU labelling experiments, mice received daily intraperitoneal injections of 2 mg BrdU (Sigma-Aldrich, Steinheim, Germany; diluted to 10 mg/ml in PBS) from day 4 post subretinal injection onwards.

Electroretinogram (ERG)

All animals were dark adapted overnight prior to ERG recordings. Animals were anesthetised, pupils were dilated using 2.5% phenylephrine and 1.0% tropicamide and ERGs were recorded using commercially available equipment (Espion E2, Diagnosys, LLC, MA). A series of scotopic recordings at different light intensities were obtained from each eye, and 0.01 cd s−1 m−2 was selected as the intensity for analysis. Photopic recordings were performed following 5 min light adaptation interval at a light intensity of 30 cd m−2. This level was also used as background light for the duration of photopic recordings. A series of photopic recordings at different light intensities were obtained from each eye, and 10 cd s−1 m−2 was selected as the intensity for analysis. After the procedure anaesthesia was reversed and the mice allowed to recover.

Reverse transcription polymerase chain reaction (RT-PCR)

Cells were washed and lysed for total RNA extraction using a silica membrane / salt buffer system (RNeasy Mini Kit, Qiagen, UK). Equal amounts of RNA were immediately reverse transcribed into cDNA using the QuantiTect Reverse Transcription Kit (Qiagen) following the manufacturer's directions. Primers for *E2F2* (5'-GCATCTATGACATCACCAACG-3' and 5'-TCAAACATTCCCCTGCCTAC-3') were used for standard qPCR reactions with a dark quencher dye (Roche, Mannheim, Germany). The PCR was run on an ABI Prism 7900HT Fast Real-time Sequence Detection System (Life Technologies, Paisley, UK). Three identical replicates were run for each sample, and the averaged C_T value was used for relative quantification using the comparative C_T method against *HPRT* as reference gene ($\Delta\Delta C_T$ method).

Western blot

Western blots were prepared as described previously[11] using the following primary antibodies: E2F2 (sc-633, Santa Cruz Biotechnology, Heidelberg, Germany), Cyclin D1 (2978, Cell Signaling Technology, Danvers, MA), GAPDH (MAB374, Merck Millipore, Darmstadt, Germany).

Immunofluorescence microscopy

ARPE19 cells grown on uncoated glass coverslips were fixed in 2% PFA for 10 min. Whole mice eyes were enucleated and fixed in 4% PFA for 1 h. For RPE flat mounts the ocular adnexa and anterior segment were removed under a dissecting microscope. Vitreous and retina were carefully detached and the remaining RPE-choroid-sclera eye cups processed for immunochemistry. Cells and eye cups were blocked in 5% normal goat serum, 1% FBS, 0.2% Triton-X in PBS. Primary antibody was incubated overnight at 4°C in blocking solution: E2F2 (1:200, #sc-632, Santa Cruz Biotechnology, Heidelberg, Germany), BrdU (1:100, #6326, Abcam, Cambridge, UK), Ki67 (1:100, #P6834, Sigma-Aldrich), ZO-1 (1:50, #40-2200, Life Technologies, Paisley, UK). F-actin was stained with phalloidin-TRITC (50µg/ml, #P1951), nuclei with DAPI (5µg/ml, #D9542, both Sigma-Aldrich). After washing three times with PBS, conjugated secondary antibodies (Alexa Fluor 488, 546, 633, Life Technologies; 1:500 in blocking solution for 1 h at room temperature) were used. Eye cups were then flattened out on a glass slide, RPE facing upwards, with a paintbrush, and covered with a glass coverslip using 40µL of fluorescent mounting medium (DAKO, Ely, UK). For retinal sections, whole eyes were embedded in O.C.T. medium (R.A. Lamb) and frozen in isopentane, precooled in liquid nitrogen. Specimens were stored at - 20 °C and 20 µm thick sections were cut using a Bright cryostat. Slides were stored at -20 °C. Sections were air dried for 10 min and marked with a hydrophobic pen before staining with DAPI. All images recorded with a confocal laser scanning microscope (Leica DM5500Q, Leica Microsystems, Wetzlar, Germany). Pictures shown are z-stack projections of multiple images covering the entire tissue depth in the z-axis.

(1) Demaison C, Parsley K, Brouns G, Scherr M, Battmer K, Kinnon C, et al. High-level transduction and gene expression in hematopoietic repopulating cells using a human immunodeficiency [correction of imunodeficiency] virus type 1-based lentiviral vector containing an internal spleen focus forming virus promoter. *Hum Gene Ther* 2002; **13**: 803-813.

(2) Yanez-Munoz RJ, Balaggan KS, MacNeil A, Howe SJ, Schmidt M, Smith AJ, et al. Effective gene therapy with nonintegrating lentiviral vectors. *Nat Med* 2006; **12**: 348-353.

(3) Dull T, Zufferey R, Kelly M, Mandel RJ, Nguyen M, Trono D, et al. A third-generation lentivirus vector with a conditional packaging system. *J Virol* 1998; **72**: 8463-8471.

(4) Bainbridge JWB, Stephens C, Parsley K, Demaison C, Halfyard A, Thrasher AJ, et al. In vivo gene transfer to the mouse eye using an HIV-based lentiviral vector; efficient long-term transduction of corneal endothelium and retinal pigment epithelium. *Gene Ther* 2001; **8**: 1665-1668.

(5) Joyce NC, Harris DL, Mc Alister JC, Ali RR, Larkin DF. Effect of overexpressing the transcription factor E2F2 on cell cycle progression in rabbit corneal endothelial cells. *Invest Ophthalmol Vis Sci* 2004; **45**: 1340-1348.

(6) Ivey-Hoyle M, Conroy R, Huber HE, Goodhart PJ, Oliff A, Heimbrook DC. Cloning and characterization of E2F-2, a novel protein with the biochemical properties of transcription factor E2F. *Mol Cell Biol* 1993; **13**: 7802-7812.

(7) Georgiadis A, Tschernutter M, Bainbridge JW, Balaggan KS, Mowat F, West EL, et al. The tight junction associated signalling proteins ZO-1 and ZONAB regulate retinal pigment epithelium homeostasis in mice. *PLoS One* 2010; **5**: e15730.

(8) Lukas J, Petersen BO, Holm K, Bartek J, Helin K. Deregulated expression of E2F family members induces S-phase entry and overcomes p16INK4A-mediated growth suppression. *Mol Cell Biol* 1996; **16**: 1047-1057.

(9) Longbottom R, Fruttiger M, Douglas RH, Martinez-Barbera JP, Greenwood J, Moss SE. Genetic ablation of retinal pigment epithelial cells reveals the adaptive response of the epithelium and impact on photoreceptors. *Proc Natl Acad Sci U S A* 2009; **106**: 18728-18733.

(10) Ali RR, Reichel MB, Thrasher AJ, Levinsky RJ, Kinnon C, Kanuga N, et al. Gene transfer into the mouse retina mediated by an adeno-associated viral vector. *Hum Mol Genet* 1996; **5**: 591-594.

(11) Han H, Kampik D, Grehn F, Schlunck G. TGF-beta2-induced invadosomes in human trabecular meshwork cells. *PLoS One* 2013; **8**: e70595.

In situ regeneration of retinal pigment epithelium by gene transfer of *E2F2*: a novel strategy for treatment of age related macular degeneration

Supplementary Material

Daniel Kampik[1,3], Ulrich FO Luhmann[1,4], Mark Basche[1], Koji M Nishiguchi[1,5], Jennifer AE Williams[2], Stephen E Moss[2], Hong Han[3], Selina Azam[1], Yanai Duran[1], Scott J Robbie[1], James WB Bainbridge[1,6], D Frank Larkin[6], Alexander J Smith[1], Robin R Ali[1,7]

[1]Department of Genetics and [2]Department of Cell Biology, UCL Institute of Ophthalmology, London, UK, [3]University Hospital of Würzburg, Department of Ophthalmology, Würzburg, Germany, [4]Current address: Roche Pharmaceutical Research and Early Development, Ophthalmology Discovery & Biomarkers, Basel, Switzerland, [5]Current address: Department of Advanced Ophthalmic Medicine, Graduate School of Medicine, Tohoku University, Sendai, Japan, [6]Moorfields Eye Hospital, [7]NIHR Biomedical Research Centre at Moorfields Eye Hospital NHS Foundation Trust and UCL Institute of Ophthalmology, London, UK

Fig. S1. Growth arrest in ARPE19 cells.

Fig. S2. LNT-E2F2 induces BrdU uptake in RPE *in vivo.*

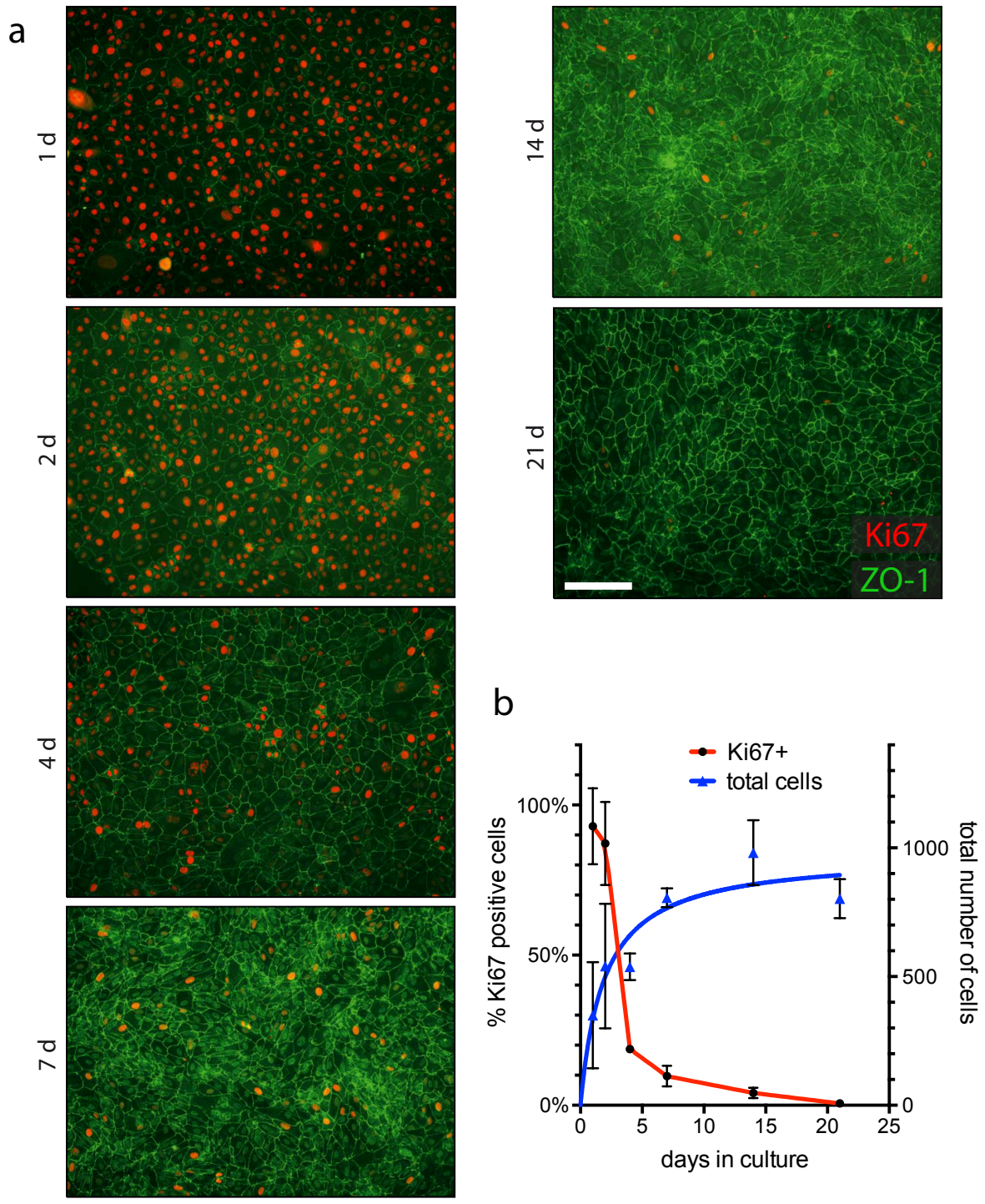

Fig. S1. Growth arrest in ARPE19 cells.

a. ARPE19 cells were cultured in starvation medium containing 1 % FCS. Over the course of 2–3 weeks, expression of tight junction marker ZO-1 (green) increased while the proportion of cells positive for proliferation marker Ki67 (red) decreased. Scale bar = 100 µm.

b. The proportion of Ki67 positive cells showed inverse correlation to the total number of cells, indicating growth arrest.

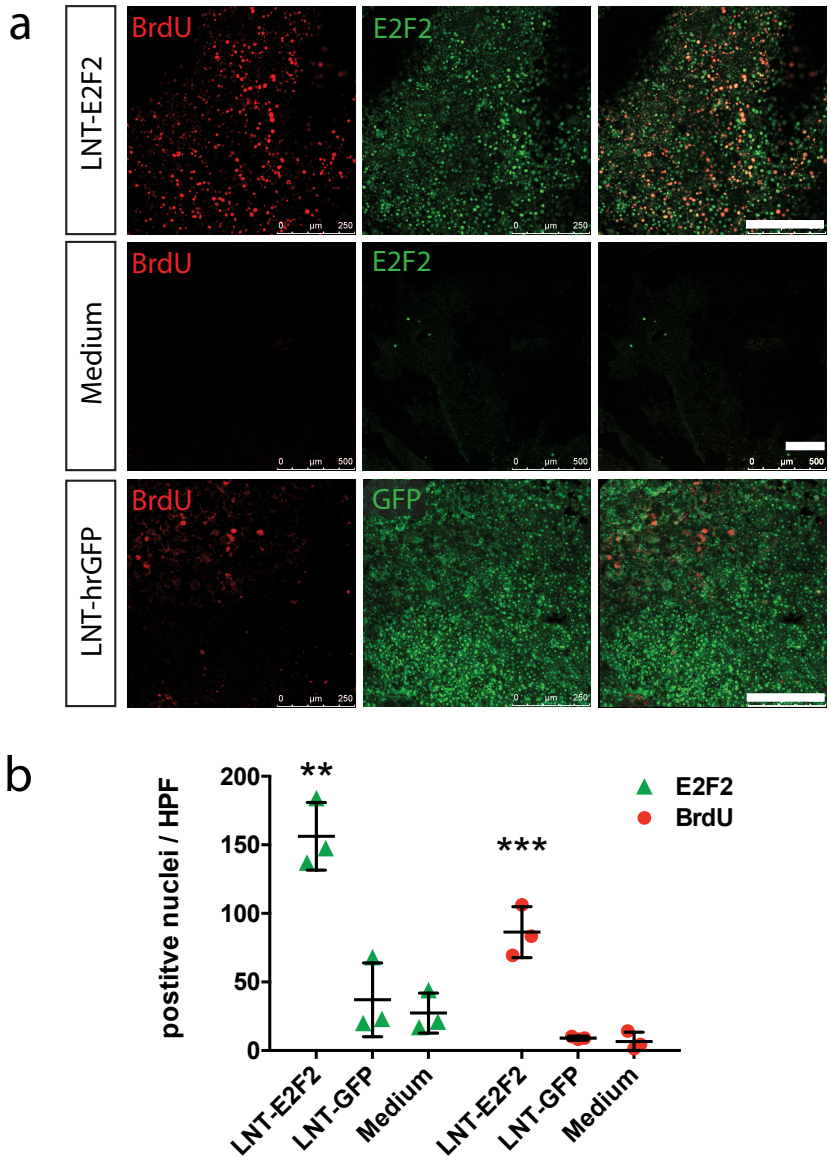

Fig. S2. LNT-E2F2 induces BrdU uptake in RPE *in vivo.*

Wildtype mice aged 12 weeks received subretinal injections of non-integrating LNT-E2F2 vector (2 x 10^5 infectious particles per eye) in the superior and inferior hemisphere of the eye. Titre matched LNT-hrGFP and medium (OptiMEM) injected eyes served as controls (n=3 eyes per group from different animals). All mice received daily intraperitoneal injections of BrdU from day 4 onwards until they were sacrificed 8 days post injection.

a. RPE-choroid-sclera was immunostained for E2F2 and BrdU and flatmounted for imaging on a confocal laser scanning microscope. Analysis included injected areas only, injection sites with trauma-related artefacts were excluded. In LNT-E2F2 injected eyes, RPE flat mounts show overexpression of E2F2 co-localizing with BrdU. Controls show very limited staining for E2F2 (medium) or BrdU (medium, LNT-GFP). Scale bar = 250 µm.

b. The LNT-E2F2 injected group showed a significant increase of E2F2 and BrdU staining compared to both control groups (P<0.0005, one-way ANOVA; ** P<0.005, *** P<0.0005 in Tukey's multiple comparisons test, no significant difference between both control groups; bars represent mean ± SD). E2F2 and BrdU positive nuclei were counted in 5 high power microscopic fields (HPF) per eye and averaged.

a

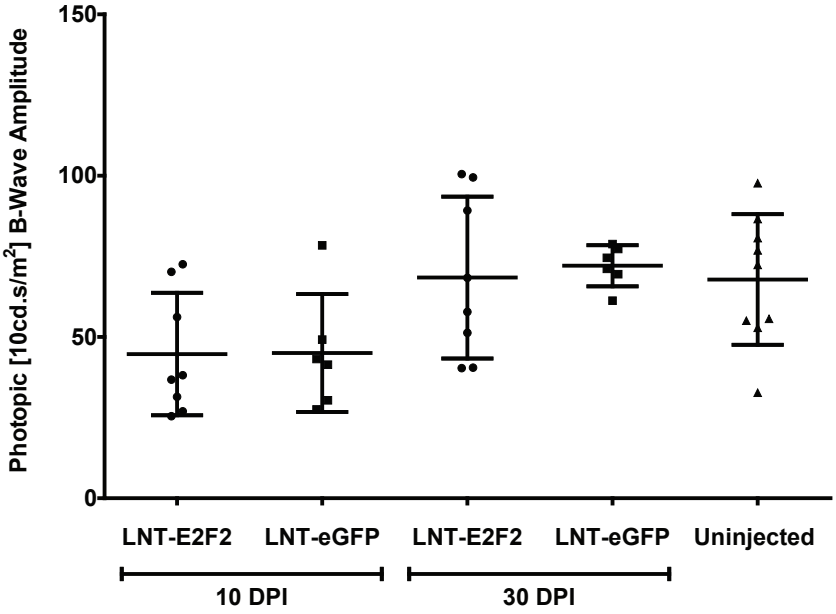
Photopic [10cd.s/m2] B-Wave Amplitude
150
100
50
0
LNT-E2F2
LNT-eGFP
LNT-E2F2
LNT-eGFP
Uninjected
10 DPI
30 DPI

b

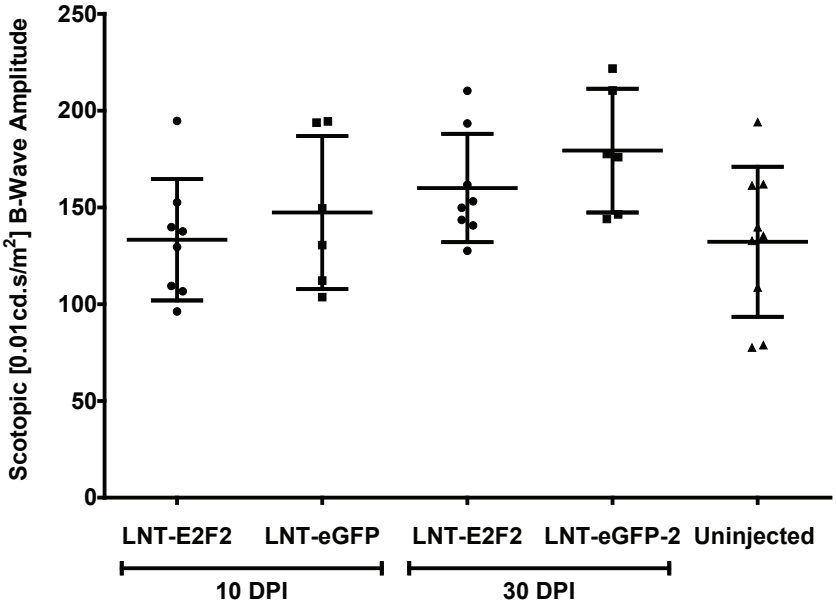
Scotopic [0.01cd.s/m2] B-Wave Amplitude
250
200
150
100
50
0
LNT-E2F2
LNT-eGFP
LNT-E2F2
LNT-eGFP-2
Uninjected
10 DPI
30 DPI

c

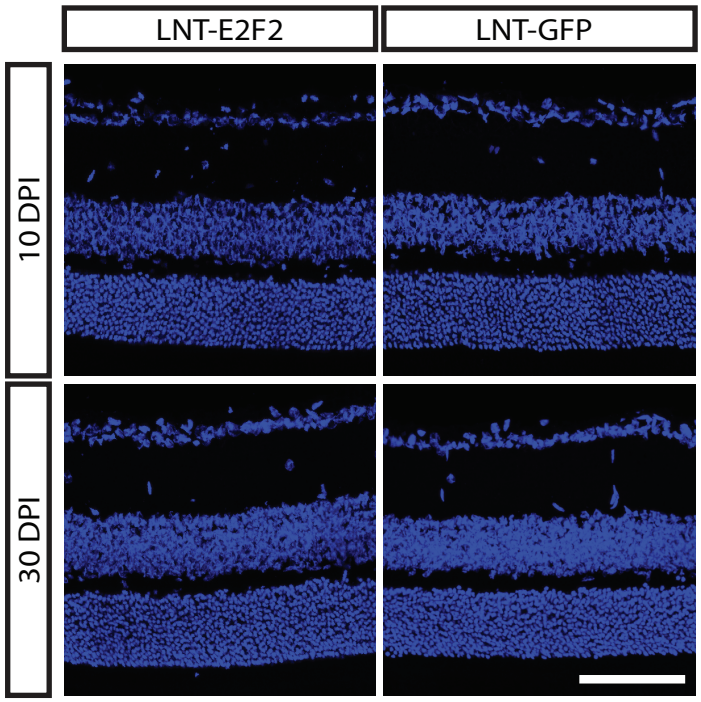
LNT-E2F2
LNT-GFP
10 DPI
30 DPI

Fig. S3. LNT-E2F2 does not affect photoreceptor function and histology.

Wildtype mice aged 8 weeks received subretinal injections of non-integrating LNT-E2F2 vector (2×10^5 infectious particles per eye) in the superior and inferior hemisphere of the eye. Titre matched LNT-GFP and uninjected eyes served as controls (n=8 eyes per group from different animals).

a. Photopic [10cd.s/m^2] ERG b-wave amplitudes in LNT-E2F2 and LNT-GFP injected eyes at 10 and 30 days post injection (DPI). Uninjected control also shown for reference. No significant differences were found (One-way ANOVA with Tukeys multiple comparisons test).

b. Scotopic [0.01cd.s/m2] ERG b-wave amplitudes in LNT-E2F2 and LNT-GFP injected eyes at 10 and 30 days post injection (DPI). Uninjected control also shown for reference. No significant differences were found (One-way ANOVA with Tukeys multiple comparisons test).

c. Representative retinal histology of LNT-E2F2 and LNT-GFP injected eyes at 10 and 30 days post injection (DPI). All images taken from the mid superior retina ~600μM from the optic nerve head. Scale bar = 100 μM.